Geoeffectiveness of three Wind magnetic clouds: A comparative study

C. J. Farrugia,[1] J. D. Scudder,[2] M. P. Freeman,[3] L. Janoo,[1] G. Lu, [4] J. M. Quinn,[1] R. L. Arnoldy,[1] R. B. Torbert,[1] L. F. Burlaga,[5] K. W. Ogilvie,[5] R. P. Lepping,[5] A. J. Lazarus,[6] J. T. Steinberg,[6] F. T. Gratton,[7] and G. Rostoker [8]

Abstract. We compare the large-scale geomagnetic response to the three magnetic clouds observed by Wind in October 1995 (OCT95), May 1996 (MAY96), and January 1997 (JAN97), studying specifically storm and substorm activity, and other global effects due to untypically large and variable solar wind dynamic pressures. Since the temporal profiles of the interplanetary parameters of the three clouds resemble one another closely, the comparison is meaningful. Using the integrated Poynting flux into the magnetosphere as a rough measure of energy input into the magnetosphere, we find relative energy inputs to be OCT95:JAN97:MAY96 = 22:11:4, with most of the accumulation in the 3-day periods occurring during passage of the $B_z < 0$ cloud phase. The peak Dst ring current indices, corrected for magnetopause currents, were in the ratio -138:-87:-38, and hence OCT95 caused a major, JAN97 a moderate, and MAY96 a weak storm. The empirical criterion derived from studies near solar maximum that a solar wind dawn-dusk electric field $\geq 5 \text{mV m}^{-1}$ lasting for at least 3 hours is necessary and sufficient to generate major storms does not hold for JAN97. Storm main phase onset coincides with cloud arrival in all three cases. The number of substorm onsets during the cloud periods were OCT95:JAN97:MAY96 = 5:3:2, with peak AL values in the ratio -1180:-1750:-570. The dayside magnetosphere was variably compressed, the largest amplitude of variation being on JAN97, where the dynamic pressure change spanned 2 orders of magnitude. MAY96 showed the least variation. The interaction of the individual clouds with the faster trailing flows had two major effects on the magnetosphere: (1) a compression of the cavity during passage of the $B_z > 0$ cloud phase and the leading edge of the fast stream; and (2) a weakening of the control of the cloud field on magnetosheath flow during the $B_z > 0$ cloud phase. In summary we find that under most of the aspects considered, OCT95 is the most geoeffective. The buffetting of the magnetospheric cavity by dynamic pressure changes was, however, strongest on JAN97. The profound differences in the magnetospheric response elicited by the clouds is found to be due to the amplitude, duration and rapidity of change of the relevant interplanetary parameters. At present, interplanetary monitors are indispensable for understanding the geomagnetic response to interplanetary structures.

[1]Institute for the Study of Earth, Oceans, and Space, University of New Hampshire, Durham.

[2]Department of Physics and Astronomy, University of Iowa, Iowa City.

[3]British Antarctic Survey, Cambridge, England, United Kingdom.

[4]High Altitude Observatory, NCAR, Boulder, Colorado.

[5]NASA Goddard Space Flight Center, Greenbelt, Maryland.

[6]Massachusetts Institute of Technology, Cambridge.

[7]Instituto de Fisica del Plasma, Universidad de Buenos Aires, Buenos Aires, Argentina.

[8]Department of Physics, University of Alberta, Edmonton, Canada.

1. Introduction

Burlaga et al. [1981] defined a magnetic cloud as a solar ejection in which (1) the magnetic field strength is enhanced with respect to ambient values; (2) the magnetic field vector undergoes a large rotation; and (3) the proton beta is low. Various studies have shown that solar ejecta in general, and magnetic clouds in particular are a leading cause of geomagnetic storms during both minimum and maximum phases of the solar cycle [*Burlaga and Lepping*, 1977; *Wilson*, 1987, 1990; *Zhang and Burlaga*, 1988; *Tsurutani et al.*, 1988, 1995; *Tsurutani and Gonzalez*, 1997; *Gosling et al.*, 1990, 1991] (see also reviews by *Burlaga* [1991] and *Farrugia et al.* [1997a]). Studying a 500-day period near solar maximum, *Gonzalez and Tsurutani* [1987] deduced that a necessary and sufficient condition for the generation of

major storms (-250 nT < Dst < -100 nT) is a solar wind dawn-dusk electric field ≥ 5 mV^{-1} lasting for at least 3 hours.

Among the magnetic clouds observed by the Wind spacecraft near the minimum phase of the solar cycle are the ejecta which passed Earth on October 18-20, 1995 (OCT95); May 27-29, 1996 (MAY96), and January 9-11, 1997 (JAN97). The aim of this paper is to compare global magnetospheric effects generated by these three clouds. These effects are associated mainly with geomagnetic storms and substorms, phenomena which are ultimately due to reconnection.

Despite the remarkably similar temporal profiles of interplanetary parameters in the respective clouds, which makes a comparison of geoeffects meaningful, we shall find that the magnetospheric responses the clouds elicit are vastly different. A further interesting feature is that all three clouds form part of compound streams, each being overtaken by a faster flow from the rear. Compared to isolated magnetic clouds, compound streams may enhance the interaction with Earth [*Burlaga et al.,* 1987]. Here, however, we shall find that the interaction affected mostly the $B_z > 0$ phase of the clouds and, as a result, it actually weakened their interaction with Earth in essential ways.

The paper is organized around the following topics: (1) comparison of the time series of corresponding cloud parameters and implications for the expected geoeffectiveness of the respective configurations; (2) estimates of energy input rates to the magnetosphere; (3) effects of dynamic pressure; (4) ring current activity; and (5) auroral electrojet activity. Taking 3-day swathes of data around each cloud enables us to include the shock (when present), the sheath region behind the shock, the cloud itself, and the interaction region and leading edge of the fast stream. We find a gradation in geoeffectiveness in roughly descending order from OCT95 to JAN97 to MAY96.

2. Interplanetary Observations

Figures 1a-1c show interplanetary proton and magnetic field data at ~1.5-min resolution for a 3-day period for each magnetic cloud under study. The data are from the SWE [*Ogilvie et al.,* 1995] and MFI instruments [*Lepping et al.,* 1995] on Wind. The horizontal axis gives time in hours starting from 0000 UT of the first day of each of the 3-day periods. The panels show from top to bottom the proton density (cm s^{-3}), bulk flow speed (km s^{-1}), and temperature (kelvin); the $B_{x,y,z}$ components of the interplanetary magnetic field (IMF) in GSM coordinates and the total field B (nanoteslas); and the IMF clock angle, α (degrees). The vertical lines in this and in Figure 2a-2c mark, from left to right, the time of arrival of the interplanetary shock at Wind (absent in MAY96), the front boundary of the cloud, the first clear B_z negative-to-positive transition inside the cloud; and the rear boundary of the cloud,

locating the latter somewhat arbitrarily at the start of the proton temperature rise. (Exact knowledge of this boundary is not important for this work.) Instead of a shock, the slow MAY96 magnetic cloud was preceded by a pressure balanced-structure [*Rosenberg et al.,* 1996] where, in high resolution, the field strengths were occasionally lower than 1 nT.

Figures 2a-2c show time series of various parameters derived from those of Figure 1a-1c: the dynamic pressure; the sum of the proton and magnetic pressures; the magnetic and proton pressures (all in nanopascals); the proton beta, the solar wind Alfven Mach number, and the so-called ϵ parameter (mW/m^{-2}). The latter, an empirical measure of the Poynting flux into the magnetosphere, is as defined by *Perreault* and *Akasofu* [1978] normalized to unit area $\epsilon = \mu_0^{-1} V B^2 sin^4(\alpha/2)$. Other aspects of OCT95 and JAN97 have been discussed by *Lepping et al.* [1997] and *Burlaga et al.* [1998].

Table 1 lists the positions of Wind. On OCT95 and MAY96, Wind was close to the Sun-Earth line and at an average radial distance of 176 R_E and 154 R_E, respectively. On JAN97 it was much closer to Earth, sunbound, and to the west of the Sun-Earth line at a mean radial distance of 110 R_E.

2.1. Time Profiles: Similarities and Differences

Figures 1 and 2 reveal clear similarities in the temporal profiles of corresponding interplanetary parameters of the three clouds. We may group these as follows:

1. All three are slow clouds, with average bulk flow speeds of 450 (JAN97), 410 (OCT95), and 370 (MAY96) km s^{-1}. Other things being equal, low solar wind speeds, v, are generally correlated with decreased magnetospheric activity [*Synder et al.,* 1963].

2. All three clouds have a long negative-to-positive B_z signature, and each is being overtaken by a faster flow. Together with v, a negative IMF B_z is the other major interplanetary quantity leading to disturbed geomagnetic conditions, consistent with the reconnection interpretation of magnetospheric activity [e.g., *Fairfield and Cahill,* 1966; *Arnoldy,* 1971]. On OCT95 and JAN97, the rectified dawn-dusk electric field exceeded 5 mV/m uninterruptedly for ~9 and ~4.5 hours, respectively; while on MAY96 the solar wind electric field peaked at 3.2 mV/m.

Clouds not being trailed by faster streams ("isolated" clouds) usually have (1) a B profile with B peaking toward the leading edge as a result of expansion, and decreasing towards the cloud boundaries by about a factor of 2 (model dependent); and (2) a front-to-back negative bulk speed gradient. By contrast, the B profiles here are flat or even enhanced toward the back, and the V profiles, except for JAN97, are flat. Following *Lepping et al.* [1997] and *Burlaga et al.* [1998], we ascribe these changes to interaction of the fast stream with the cloud. Besides compressing the field, this interaction has also increased n. The n panels of Figures 1a-1c
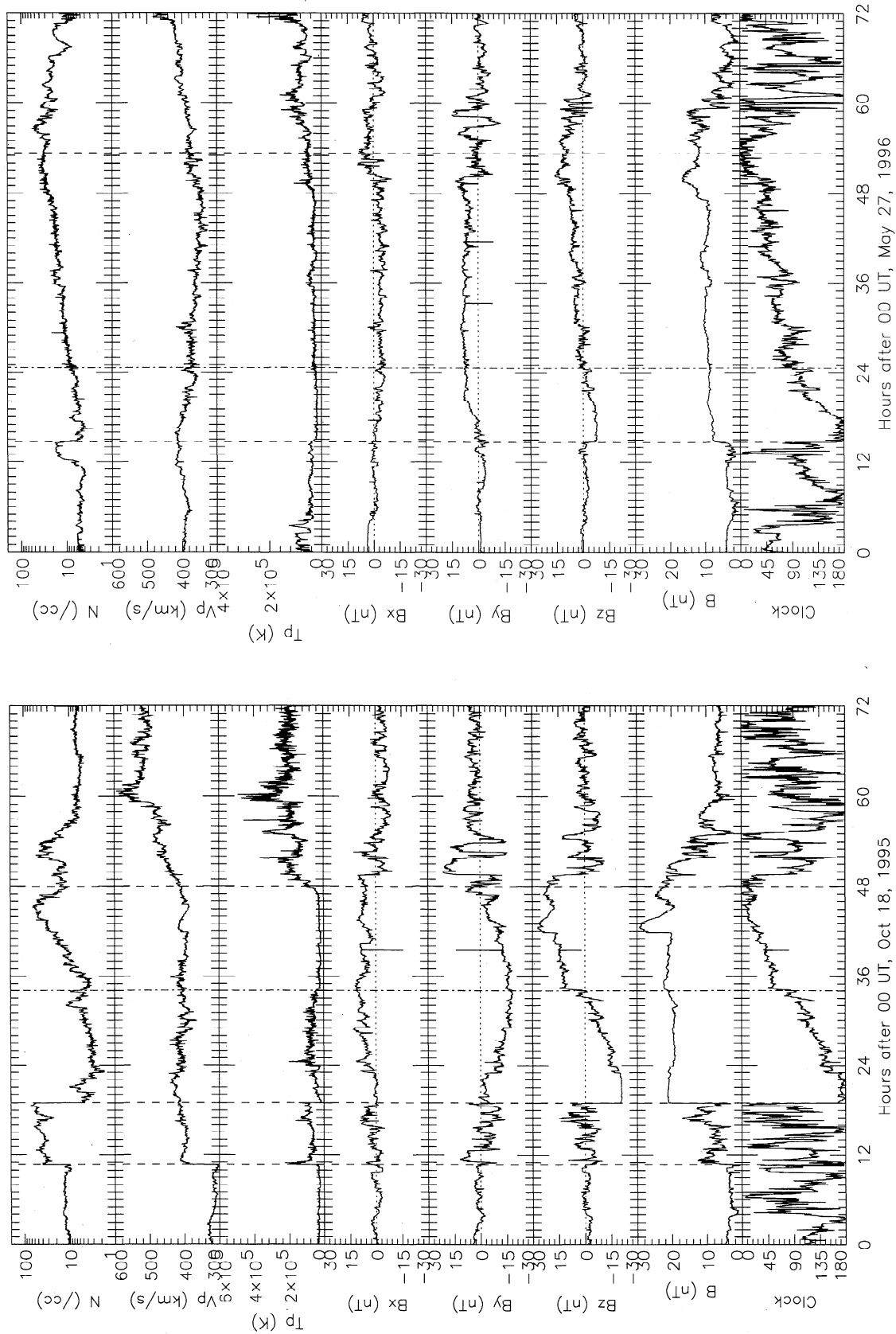
Figure 1. Proton and magnetic field data for a 3-day interval for (a) OCT95, (b) MAY96, and (c) JAN97, respectively. The panels show from top to bottom the proton density, speed, and temperature; the GSM components of the magnetic field and the total field; and the clock angle of the interplanetary magnetic field. The vertical lines in this and all other figures in this paper correspond to, from left to right, the Wind universal time of arrival of the interplanetary shock (absent on MAY96), the cloud front boundary, the first clear B_z negative-to-positive polarity transition inside the cloud, and the rear boundary.
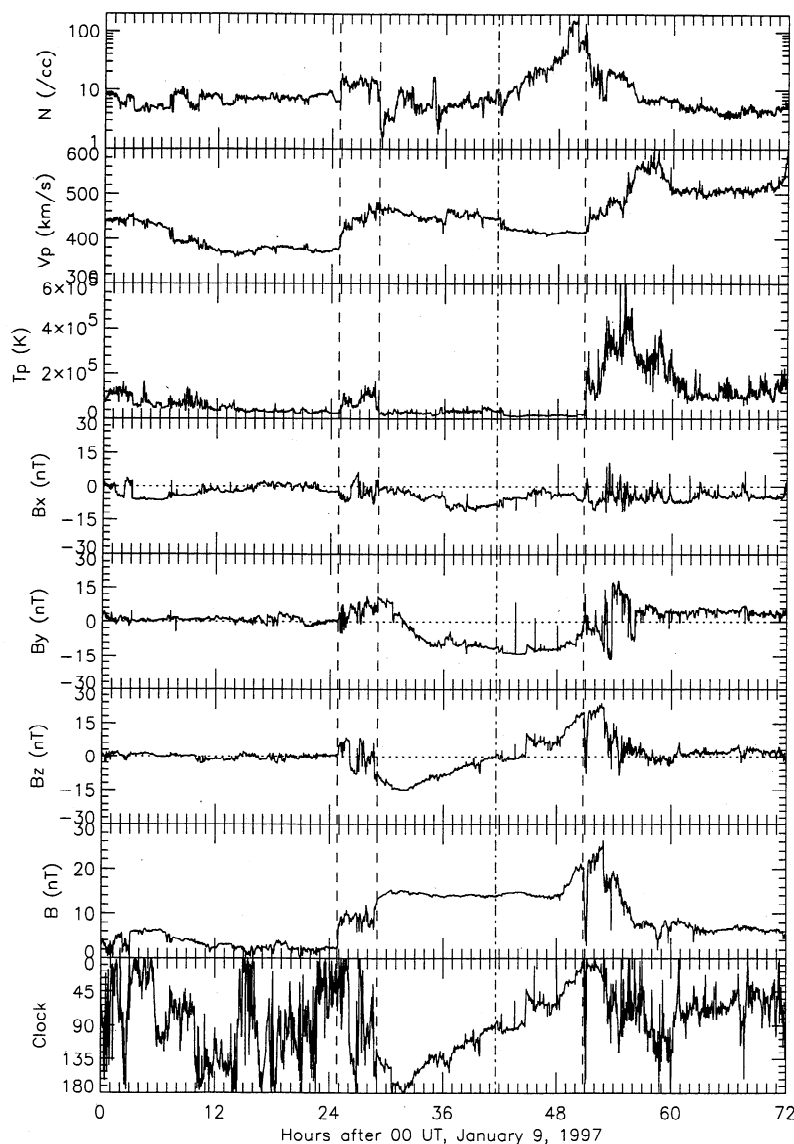
Figure 1. (continued)

show that the effect is most pronounced after the B_z transition, at which the positive gradient in n increases sharply and across which n increases by about an order of magnitude.

3. All three magnetic cloud fields have significant B_x and B_y components. There are various magnetospheric effects induced by these two IMF components [*Cowley*, 1981, 1991; *Freeman et al.*, 1990, 1993; *Knipp et al.*, 1993], particularly dawn-dusk asymmetries of ionospheric flows (B_y) and regulation of topology in reconnection poleward of the cusp (B_x) [e.g. *Crooker*, 1992]. Detailed studies of the magnetosphere response to the individual clouds should thus yield interesting results [see, e.g., *Scudder et al.*, 1996].

4. All three clouds are preceded by a ramp of high dynamic pressure (due mainly to the high density) of a few hours' duration. At onset, a remarkable feature of these Wind clouds is a rapid release of this pressure occurring closely in time with a large and abrupt south-ward turning of the field. The resulting rapid inflation of the magnetospheric cavity and large rate of energy influsion lead to a highly dynamic magnetospheric state. The most impulsive onset occurs on OCT95, where the dynamic pressure drops precipitously from 18 to 1.5 nPa as the field rotates by 180° in 6 min. On JAN97, the dynamic pressure drop (from ~5.5 to ~0.4 nPa) actually followed the ~120° southward field rotation by ~12 min. Since after cloud arrival, B stays fairly constant and V varies little, the power input to the magnetosphere measured by ϵ is determined largely by the IMF clock angle variation. Because of the peculiarities of the onsets, most of the energy and momentum coupling with the magnetosphere occurs during the early hours of cloud passage.

5. In all three clouds, the clock angle varies over its whole range of definition. It does not increase monotonically, however, because the cloud field does not rotate smoothly [e.g., *Janoo et al.*, 1998]. There are also
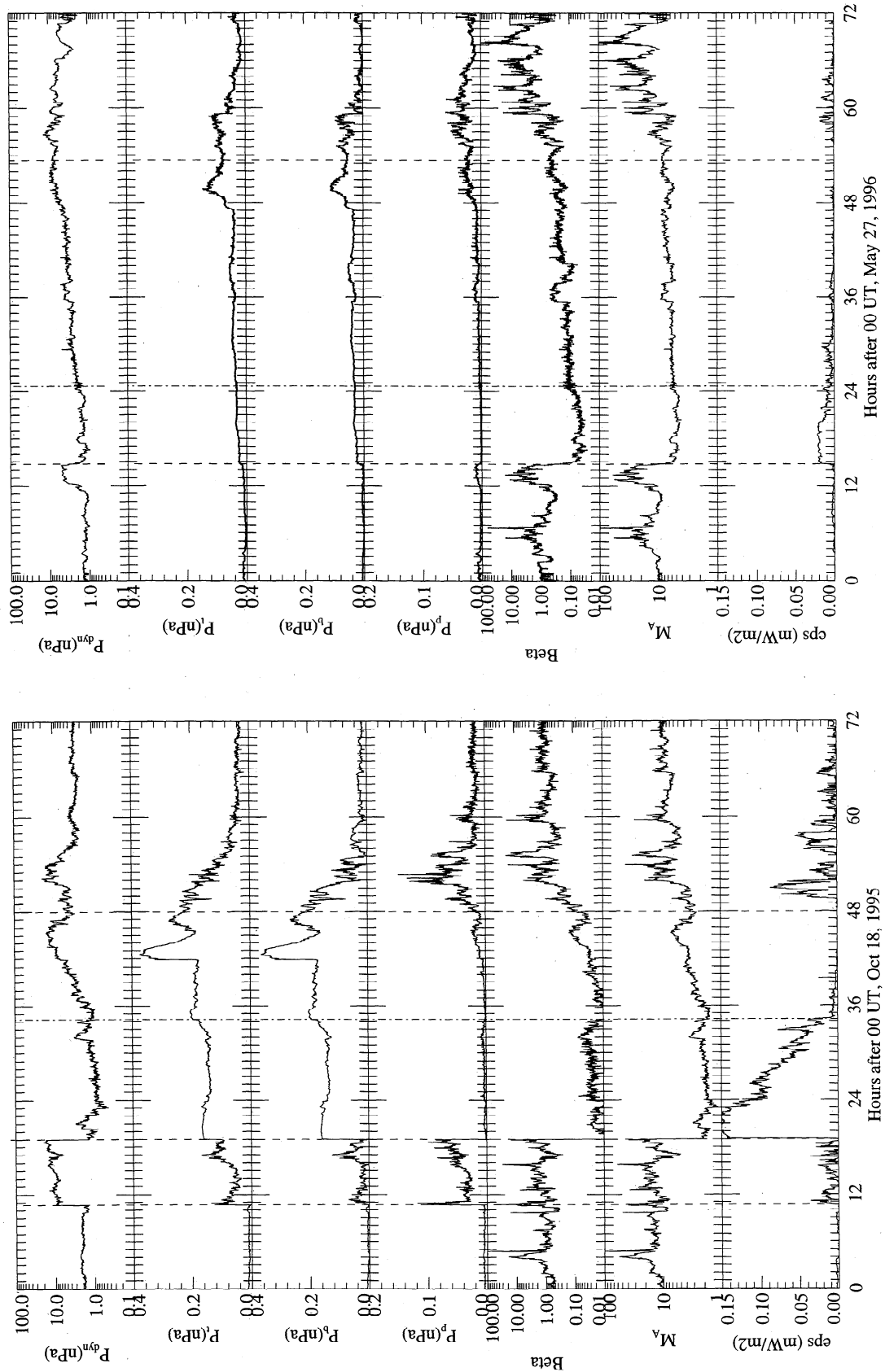
Figure 2. Panels show from top to bottom the dynamic pressure, the sum of the proton and magnetic pressures, the magnetic pressure, the thermal pressure, the proton beta, the Alfvén Mach number, and the ϵ parameter: (a) OCT95, (b) MAY96, (c) JAN97.
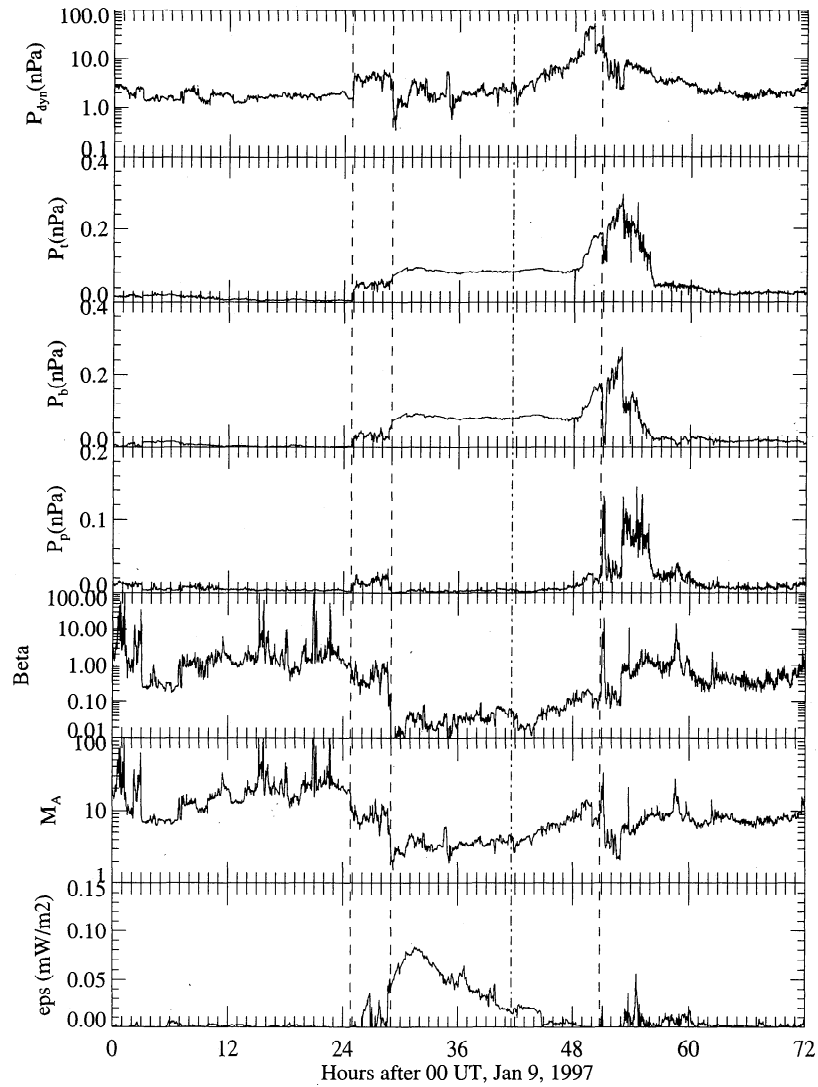
Figure 2. (continued)

Table 1. Position of Spacecraft

Universal Time	Position Vector	Radial Distance, R_E
Oct. 18 - 20, 1995		
0000 UT, Oct. 18	(174.4,-5.0,-13.7)	175.0
0000 UT, Oct. 19	(175.4,-3.4,-13.2)	176.0
0000 UT, Oct. 20	(177.0,-0.2,-12.0)	177.4
May 27 - 28, 1996		
0000 UT, May 27	(147.7,-11.8,-9.3)	148.4
0000 UT, May 28	(152.0,-9.4,-9.9)	152.6
0000 UT, May 29	(156.0,-7.1,-10.4)	160.3
Jan. 9 - 12, 1997		
0000 UT, Jan. 9	(75.5,-61.1,-2.2)	97.2
0000 UT, Jan. 10	(84.7,-59.5,-3.4)	103.6
0000 UT, Jan. 11	(93.2,-57.5,-5.6)	109.6
0000 UT, Jan. 12	(100.9,-55.4,-5.6)	115.2

episodes of many hours' duration at the clouds' rear where the clock angle is very small. Interplanetary conditions are then ideal for exciting the Kelvin-Helmholtz (KH) instability at the dayside magnetopause.

6. OCT95 and JAN97 have extremely low proton β: an average of 0.03 before the B_z transition, increasing gradually by almost an order of magnitude toward the cloud's rear. The proton β values on MAY96 are higher with a similar increasing trend toward the rear.

Studies of reconnection at the low latitude magnetopause indicate that the occurrence of reconnection-associated high speed flows at the magnetopause are inversely correlated with the magnetosheath beta [Paschmann et al., 1986]. Low beta has thus been tentatively suggested to favour reconnection [Paschmann et al., 1986; Phan et al., 1996]. While the beta in these studies is that near the reconnection line at the magnetopause, one might nonetheless expect that, in view of the extremely low solar wind values, particularly on JAN97 and OCT95, the relevant magnetosheath beta when these clouds are convected into the magnetosheath will also be low.

7. The solar wind values of the Alfven Mach number, M_A ($M_A^2 = \mu_0 \rho v^2 B^{-2}$, where ρ is the mass density) before the shock/pressure balanced-structure are generally high for all three clouds ($\geq \sim 10$). During the cloud $B_z < 0$ phase, they are low and fairly constant (2-3 for OCT95 and ~ 4 for JAN97 and MAY96). During the $B_z > 0$ phase, M_A increases to values 7-10 because the increase in B^2 (with respect its behavior in isolated clouds) is offset by the larger increase in n. The effect is most pronounced for JAN97 and MAY96. In isolated clouds, such as the January 1988 magnetic cloud, $M_A \sim 3$ throughout the entire cloud passage [Farrugia et al., 1995]. Low M_A values imply a strong control of magnetosheath flow by the IMF, leading to wide plasma depletion layers [Farrugia et al., 1995, 1997b]. For the present examples, however, only a thin (~ 0.5 R_E) plasma depletion layer adjacent to the sunward side of the magnetopause is to be expected, while the rest of the magnetosheath flow may be treated by gas dynamics to good approximation. We conclude that the control exerted by these clouds' magnetic fields on magnetosheath flow during the $B_z > 0$ cloud phase has been weakened by their interaction with the faster stream.

In summary the time profiles of corresponding parameters characterizing the three clouds are very similar. The differences concern mainly the different cloud durations, the different speeds, the duration of $B_z < 0$ phase and the different range of negative B_z, differences in the sharpness of onset, level of density fluctuation, rapidity of dynamic pressure changes, and clock angle profiles. Nonetheless, these qualitative differences lead to profound differences in the geomagnetic response elicited by the individual clouds.

2.2. Estimates of Energy Inputs to Magnetosphere

As a general prediction on the geoeffectiveness of these three configurations, based on the upstream measurements just described, we integrated the Poynting flux, given by the ϵ parameter, over time for each of the 3-day periods. Particularly under disturbed magnetospheric conditions, this integral correlates well with the energy input into the magnetosphere, where it appears as Joule heating, ring current dissipation and electrojet activity [Perreault and Akasofu, 1978; Baker et al., 1983; Akasofu, 1981; Stern, 1984]. The thin line in Figure 3 reproduces the variation of ϵ, and the thick line shows its integral over time. We work in terms of unit area. (For easy conversion, we note here that 1 Wm^{-2} = 2 x 10^{15} W over a 7 R_E x 7 R_E magnetopause; and 1 J m^{-2} = 2 x 10^{15} J = 2 x 10^{22} ergs.)

Maximum values of ϵ are in the ratio 14:8:2 for OCT95:JAN97:MAY96. The maximum value is reached very quickly on OCT95 and MAY96 but less so on JAN97. The total energy entering the magnetosphere over the three 3-day periods are ~ 22:~ 11:~ 4 for OCT95: JAN97:MAY96. Most of this energy enters during the $B_z < 0$ phase of cloud passage, and, indeed, 75% of the total energy is accumulated within ~ 9 hours of cloud arrival on OCT95 and JAN97 and within ~ 15 hours on MAY96. The accumulated energy during the cloud intervals alone are in the ratios 43:22:7. As a fraction of the total energy over the 3-day periods, the energy input during the MAY96 cloud is proportionately the highest, reflecting more the quiet conditions around cloud passage than the strength of the cloud-magnetosphere coupling. While behind the cloud, energy is accumulated at a much reduced rate; on OCT95 and JAN97 there is a second energy infusion during the passage of the interaction region between the cloud and the following fast stream. There is also some energy input to the magnetosphere during passage of the sheath regions on OCT95 and JAN97, and the amounts are comparable (4:3), even though the JAN97 sheath is only about half as wide.

3. Magnetosphere Compression

Figure 4 shows the variation in time of the radial position of the subsolar magnetopause (R) during passage of the three clouds, computed from pressure balance with an assumed 4% α/H^+ density ratio. The subsolar position is referred to its statistical average, 11 R_E [Fairfield, 1971].

At the start of the interval, all subsolar magnetopauses are close to the nominal position. At the end of the interval, they are in all cases displaced earthward by ~ 1.5 R_E. In between, there is much variation, of maximum amplitude ~ 8 R_E. Considerable magnetopause com-
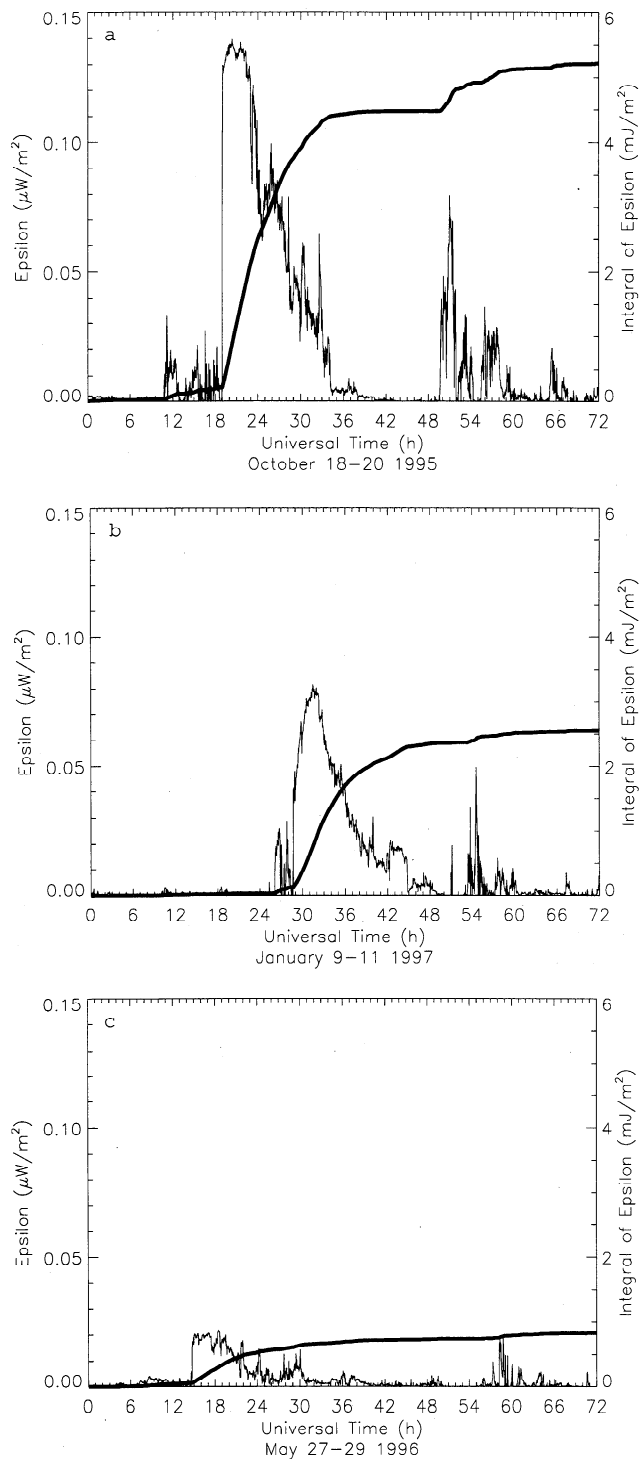
Figure 3. The variation of the ϵ parameter during each of the 3-day intervals (thin line) and its time integral (thick line) for (a) OCT95, (b) JAN97, and (c) MAY96.

pression results from sheath passage, that on OCT95 being about twice as large (3.8 versus 2.2 R_E) as on JAN97. The compression during the pressure-balanced structure on MAY96 is comparable to that on JAN97. The sudden release of dynamic pressure at cloud onset returns the subsolar position to near its nominal values on OCT95 and MAY96, but on JAN97 it is momentar-

ily displaced by ~ 3 R_E sunward, signalling the largest inflation of the magnetosphere.

During passage of the $B_z < 0$ phase of the clouds, the subsolar position given in the figure is an overestimate since we do not include dayside erosion. *Petrinec and Russell* [1993] estimate an earthward magnetopause displacement of 1 R_e for every 7.4 nT of southward B_z, i.e., in our case $\sim$1-2.5 R_e, the largest on OCT95 and the smallest on MAY96. In both phases of cloud passage there is thus considerable magnetospheric compression.

Behind the cloud, the pressures tend to stabilize, but, in view of the high speed of the streams overtaking the clouds, the magnetopause is compressed with respect to values at the start of the 3-day intervals, as noted above.

In addition to the slow and large-amplitude changes in the dynamic pressure, we must also consider the rapid, low-amplitude fluctuations of this quantity. Plate 1 shows the power spectral density of these fluctuations. For this analysis, the dynamic pressure was divided into overlapping sections, and each section was linearly detrended and windowed using a Hanning window. The Nyquist frequencies for OCT95, JAN97, and MAY96 were 4.4×10^{-3}, 6.5×10^{-3}, and 3.6×10^{-3} Hz, respectively. The blue, red, and green traces refer to results for OCT95, JAN97, and MAY96, respectively. It can be seen that for all frequencies corresponding to periods from $\sim$6.9 hours to $\sim$3 min the power spectral density in the JAN97 fluctuations exceed those of the other two clouds. It follows that the effect of the dynamic pressure will play a predominant role in the interaction of JAN97 with Earth. For most of the lower frequencies, the dynamic pressure fluctuations on OCT95 have more power than those on MAY96. At the high-frequency, low-period end of the spectrum, the power spectral densities tend to be similar.

4. Ring Current Activity

To study ring current activity, 18 stations with magnetic latitude (MLAT) $\leq 40°$ were used for calculating the Dst on OCT95, 15 on MAY96, and 13 on JAN97. To find the contribution of the ring current to the Dst (Dst^*) we took into account a quiet time correction of 20 nT and a correction for magnetopause currents, following *Burton et al.* [1975]. We did not, however, correct for the conductivity of the solid Earth [*Stern*, 1984, and references therein].

4.1. OCT95

Figure 5a shows the Dst and Dst^* values (diamond and starred symbols, respectively) for OCT95. We timed the delay for signals at Wind to influence the ring current by comparing the arrival of two related, impulsive features: the dynamic pressure release at cloud onset on Wind and the large and sharp drop in raw Dst values. This gave a time delay of 44 min. Since Wind is at practically stationary (Table 1), we lagged
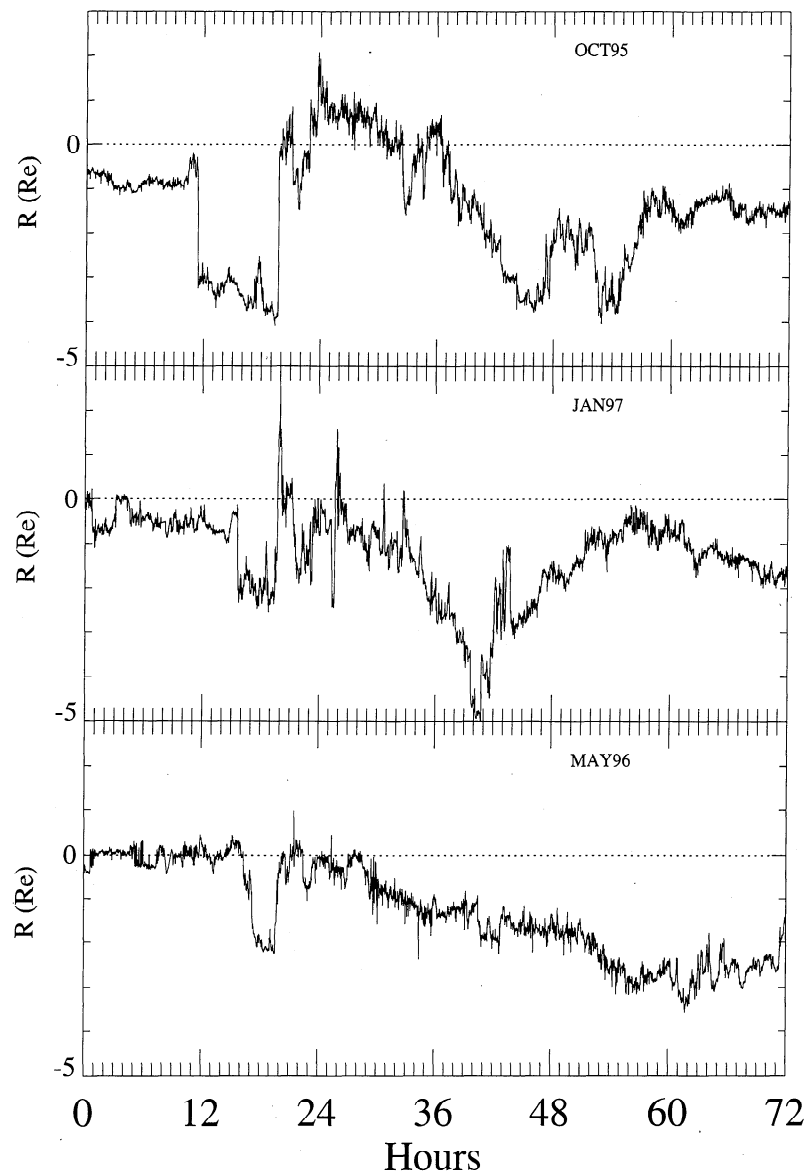
Figure 4. The subsolar magnetopause position, as given by pressure balance assuming a 4% alpha-to-proton density ratio, referred to its average statistical location, 11 R_E. Effects of dayside erosion are not included.

all interplanetary readings by this value for the entire 3-day interval. Five-min averages of the magnetopause currents were then formed, similarly lagged, and subtracted from the raw Dst values.

The following points may be made: (1) The 8-hour-long passage of the sheath after the storm sudden commencement is accompanied by moderate ring current activity. (2) The main phase of the storm starts on arrival of the front cloud boundary. The growth of the main phase is rapid, with a Dst^* minimum of -135 nT reached within 3.25 hours. The duration of the growth of the main phase coincides exactly with the interval of smooth and almost constant, negative B_z at the start of cloud (B_z = -19.9 ± 0.2 nT; Figure 1a) (3) Average Dst^* values ~-120 nT are maintained for ~ 6 hours, during which the solar wind electric field is larger than

5 mV/m. (4) A rapid recovery sets in ~4.5 hours before the B_z transition inside the cloud, is momentarily reversed by a further injection, resumes its fast rate for some hours, and is then completed by the time the rear edge of the cloud passes by. The further injection correlates well in time with a decrease of negative B_z at hour 32.8 (Figure 1a, B_z panel). (5) Thereafter, further moderate activity resumes, and quiet conditions are not reached until October 26. This activity is due to the intermittent $B_z < 0$ activity in the Alfven waves in the fast stream [*Lepping et al.*, 1997] (6) The cloud dawn-dusk electric field was ≥ 5 mV/m for ~ 9 hours. Since the magnetic storm was of major intensity, the criterion derived by *Gonzalez and Tsurutani* [1987] for solar maximum conditions is satisfied. *Jordanova et al.* [1998] simulate the ring current development during the
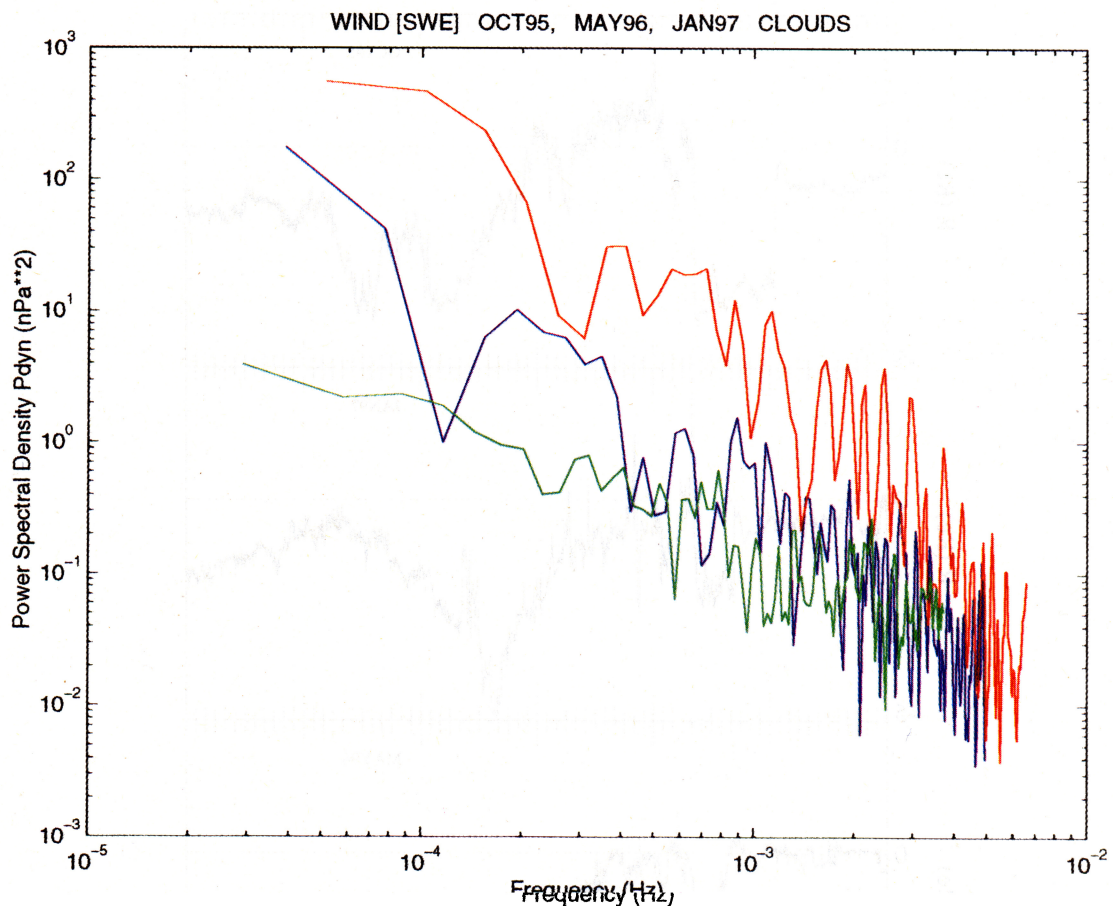
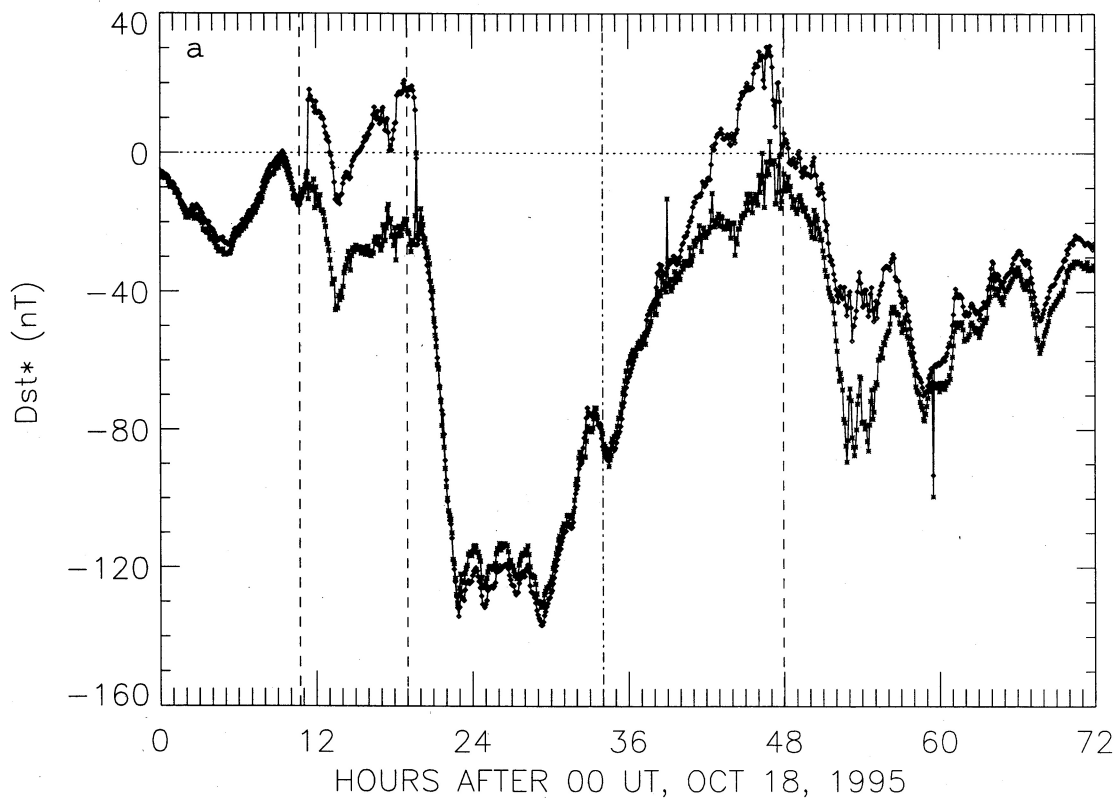**Plate 1.** The power spectral density of the dynamic pressure variations for OCT95 (blue), JAN97 (red), and MAY96 (green).

Figure 5. The ring current contribution to the Dst index, Dst^*, after quiet time magnetopause currents corrections are made, is shown by starred symbols. The raw Dst values are shown by diamond symbols. The data are 5-min averages. Appropriate corrections for signal transmission have been included. (a) OCT95; (b) JAN97; (c) MAY96.
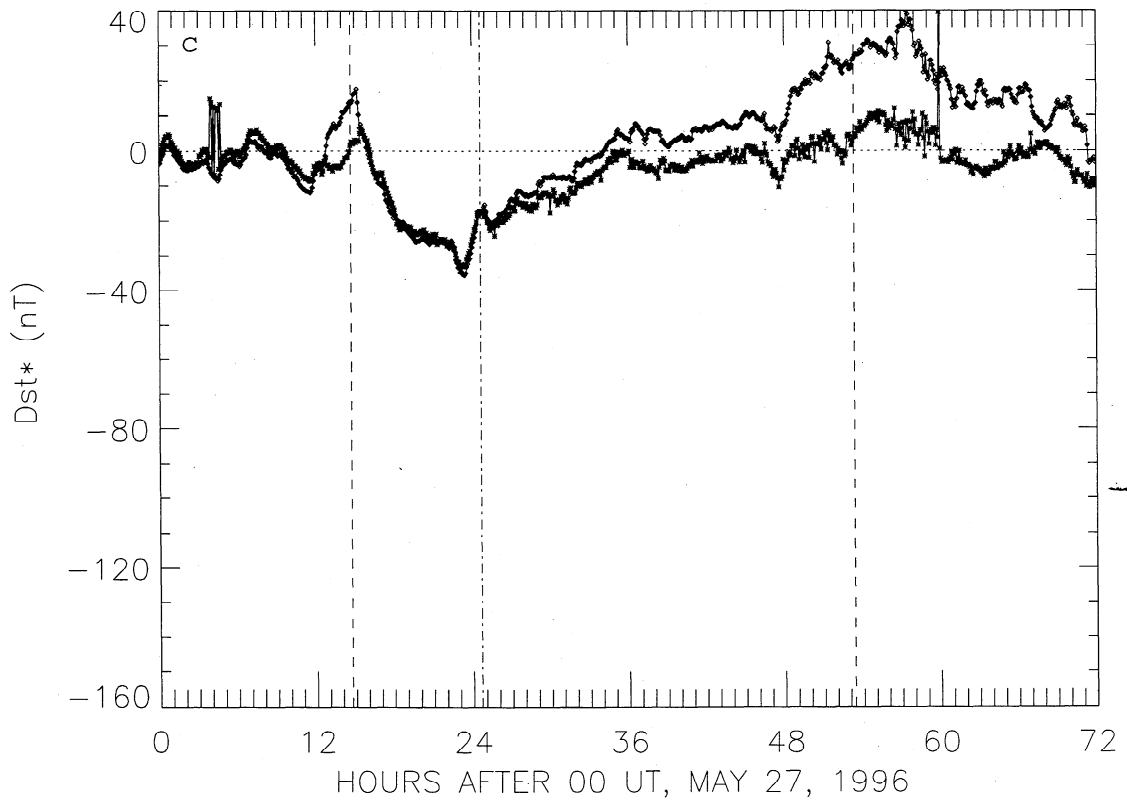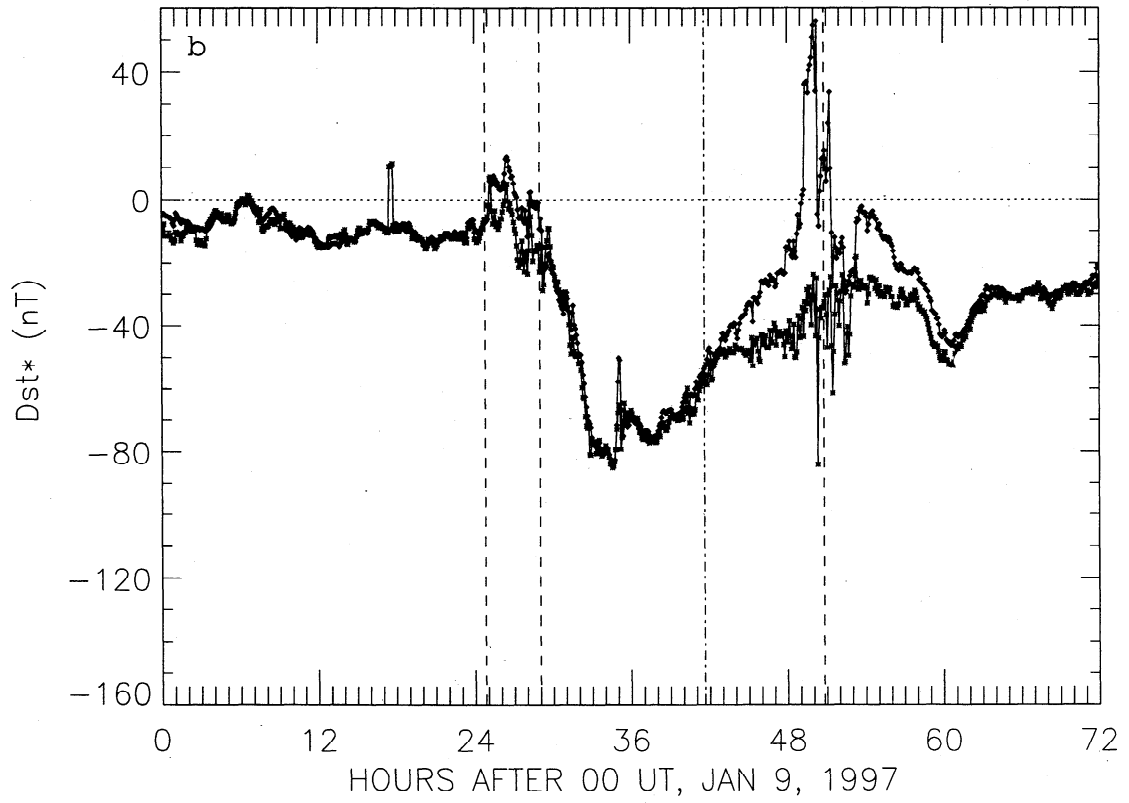
Figure 5. (continued)

two storms on October 18 - 26, 1995, using the bounce-averaged kinetic model of *Jordanova et al.* [1997]. A major contributor to the ring current energization in this period is the presence of intervals of superdense plasmasheets at geostationary orbit, i.e., plasma sheet density in excess of ~ 1.5 cm^{-3}, one burst during the main phase of the storm, and a second burst during the first Dst^* minimum after cloud passage [*Jordanova et al.*, 1998] when the solar wind density is high and the IMF B_z is mainly negative. The role of superdense plasma sheets for energizing the ring current population has been investigated by *Borovsky et al.* [1997].

4.2. JAN97

For the early part of JAN97 cloud passage the signal delay can be estimated by comparing the dynamic pressure rise at the shock driven by the cloud and the impulsive increase in the Earth's field at low latitudes (storm sudden commencement (ssc)) as done by *Villante et al.* [1997]. This method gives an 18-min delay. For the later part of cloud passage we compare the sharp dynamic pressure rise at the rear of the cloud with an impulsive rise in the raw Dst values. This yields, in turn, a 26 min delay, an increase caused by Wind receding from Earth (Table 1). In producing Figure 5b we take the average of these (22 min). At the rear of the cloud between hours 46 and 56, solar wind variations occur on a scale comparable to the 5-min resolution of the Dst data. For these hours we took the delay to be 26 min.

We summarize the main observations as follows: (1) Just as on OCT95, the main phase of the storm starts on cloud arrival and takes about 3.5 hours to complete. (2) The minimum Dst^* is -83 nT, i.e., a moderate storm. Nonetheless, the solar wind electric field exceeded 5 mV/m for $\sim$ 4.5 hours. In this case, the criterion of *Gonzalez and Tsurutani* [1987] for the generation of major storms is not satisfied. (3) As on OCT95, minimum Dst^* is reached after minimum cloud B_z is attained, by about 2 hours in this case. (4) Storm recovery starts just prior to the B_z transition inside the cloud and, unlike OCT95, fails to be completed by the end of cloud passage. (5) The large dynamic pressure increase at the rear of the cloud (Figure 2c) failed to enhance ring current activity. This is primarily because, despite solar wind densities in excess of 150 cm^{-3} (Figure 1c), there was no evidence of a superdense plasma sheet and the plasma sheet density remained of order 1 cm^{-3} (J. E. Borovsky, private communication, 1997). The absence of superdense plasma is probably due to the northward IMF orientation at this time, which precludes entry into the magnetosphere [*Borovsky et al.*, 1997]. (6) There is some moderate activity on January 11, but this dies down on the following 2 days.

4.3 MAY96

For MAY96 (Figure 5c), signal time delay is $\sim$40 min. In contrast to OCT95 and JAN97, the activity is weak

throughout, with the only very moderate activity just prior to the B_z transition. Complete recovery and even positive Dst^* values are attained around the passage of the rear boundary of the cloud.

Summarizing ring current activity caused by the three clouds, we find a major followed by a moderate storm on OCT95, moderate ring current activity on JAN97, and weak activity on MAY96.

5. Auroral Electrojet Activity

5.1. AE and AU Indices

To compare the general auroral and substorm activity, we use a multistation determination of the AE, AL, and AU indices. The coverage, from stations between 55° and 76° MLAT, is as follows: 61 stations for October 18-19; 21 stations for October 20; 61 stations for JAN97, and 68 stations for MAY96. Five min average values are shown in Figure 6. (The AU index is shown by the dashed line.) The magnetosphere response evident in Figure 6, include further, "internal" delay time lags during which the magnetotail stores energy/magnetic flux from the dayside prior to substorm onset.

A comparison of the corresponding AE indices shows that (1) during passage of the $B_z < 0$ phase of the clouds, the AE activity in OCT95 and JAN97 are fairly comparable, but there are longer intervals with $AE > 1000$ nT in OCT95. MAY96 has a much lower level of AE activity, which never reaches 1000 nT.

For OCT95 and MAY96, there is much lower activity ($AE < 400$ nT) in the subsequent $B_z > 0$ phase of the cloud, while on JAN97 there is a further AE burst in the period 42.5-44.5 hours, during a time when the clock angle exceeds 90° for an extended period of time (Figure 1c). (Recall that the clock angle variation is not smooth.) In OCT95, after 2 hours of activity (i.e., 1.25 hours after estimated passage at Earth of the B_z transition inside the cloud), extraordinarily quiet AE conditions ($AE \sim$100 nT and constant) prevail which last to well after cloud passage. Referring to Figure 1a, this means that reconnection at the dayside magnetopause, the presumed cause of this activity, stopped fairly abruptly when the IMF clock angle decreased below $\sim$50°. Equating roughly the IMF clock angle with the local magnetic shear at the low latitude magnetopause, 50° is around the lower end of the scale characterizing the local magnetic shear for which reconnection at the low-latitude magnetopause has been observed to occur [*Phan et al.*, 1996].

AE values in the $B_z > 0$ nT phase of MAY96 go up to $\sim$200 nT. The AE profile reflects the fact that clock angle does not decrease monotonically (see Figure 1a). The small but clear AE increases during hours 28-31, 37, and 38-39 correlate very well with increases in the clock angle seen at Wind about 50 min to 1 hour earlier (Figure 1b).

AE activity is moderate during passage of the OCT95 cloud sheath with an average AE of $\sim$500 nT and with

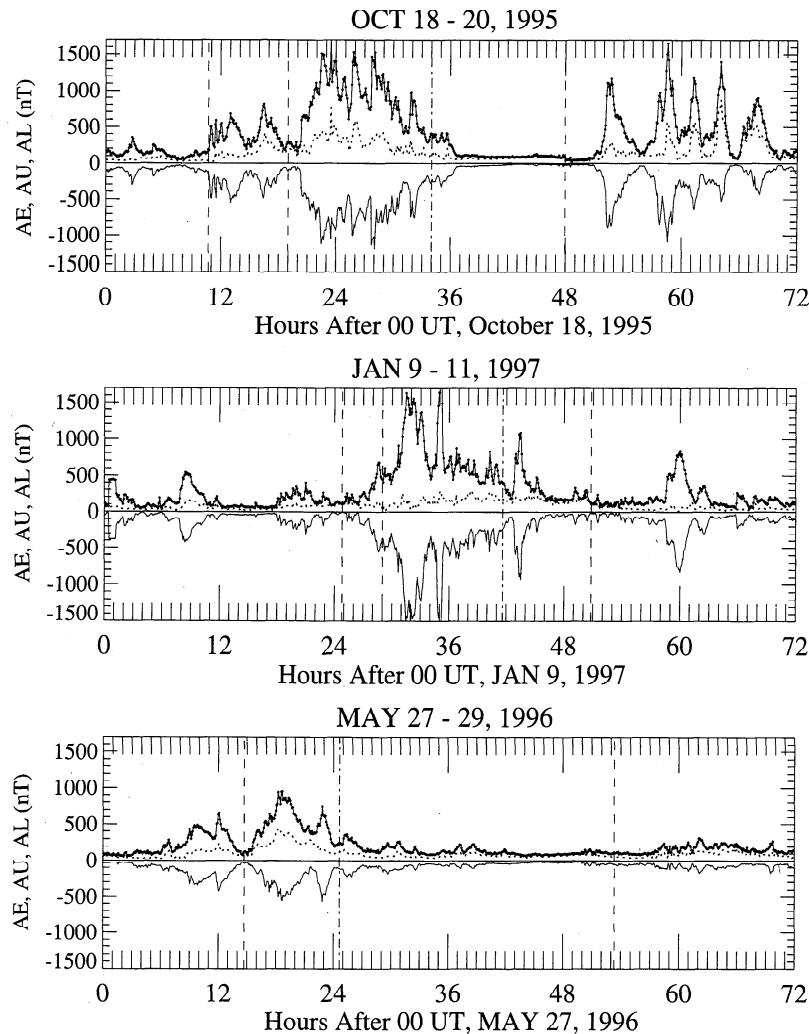**Figure 6.** AL, AU (dashed), and AE indices for the three intervals studied. The vertical lines are drawn at Wind times. (top) OCT95, (middle) JAN97, (bottom) MAY96.

two bursts of enhanced activity. Activity during the passage of the sheath of the JAN97 magnetic cloud is weak but increases toward the latter end of sheath passage to over 500 nT. During the passage of the pressure-balanced structure preceding MAY96, the activity decreases steadily to very low values.

Large differences are elicited by passage of the leading edges of the high-speed steams. There is only minor activity on MAY96, and one burst of activity on JAN97 centered at hour 60 where the clock angle (Figure 1c) exceeds 90°. On OCT95, however, the activity, though more sporadic than in the cloud, reaches intensities comparable to those during cloud passage. These are examples of high-intensity, long-duration, continuous auroral activity (HILDCAAs) whose cause are Alfven wave trains riding on the faster stream [*Tsurutani and Gonzalez*, 1987; *Lepping et al.*, 1997].

To compare substorm activity, we consider the AL index. We note first that indices such as AE and AL can only give a broad indication of the actual level of substorm activity and what follows should not be considered as a definitive picture of the prevailing substorm

activity, but only a general indication. One would require more extensive data to obtain maximum reliability in the identification of substorm onsets, since, e.g., small bays may be overlooked.

As regards the number of substorm onsets, and not counting what look like pseudo breakups, on OCT95 there are about equal numbers (5) in the cloud and in the interaction region behind the cloud over a comparable length of time. On JAN97 there appear to have been fewer substorm onsets: three clear onsets during cloud passage, and 1 in the interaction region behind the cloud, the latter corresponding to the $B_z < 0$ interval in Figure 1c around hours 57-60. On MAY96 there are two clear substorm onsets during the $B_z < 0$ phase. What appear to be two other small injections in the "$B_z > 0$" phase are likely to be intensifications of the ionospheric convection ($DP2$) electrojets resulting from short-duration fluctuations in the cloud clock angle. In the wake region, there is a minor intensification of the westward electrojet current when B_z oscillates about 0 at low amplitude (Figure 1b). In summary we find that AE activity is more sustained and the number of sub-

storms greater in OCT95 than in JAN97. MAY96 is very weak in terms of AE activity.

So, we have shown that a single class of interplanetary phenomena, a magnetic cloud, can vary greatly in its global auroral geoeffectiveness: all magnetic clouds may be magnetic flux ropes, but their size, orientation, relative strength of axial and azimuthal field components, etc. are different and these properties are equally important in determining their geoeffectiveness. Thus, in the forcasting of a so-called space weather, one cannot reliably predict the geoeffect of a solar event from the time of its birth on the Sun. We return to this point in the discussion section.

5.2. Latitudinal Chain of Magnetometers

Of equal importance to space weather forecasting is the concentration of the global energy in specific regions of the magnetosphere and ionosphere, and whether such areas are proximate to a satellite, an HF radio link, a national power grid, etc. The AE indices are not designed for this purpose since they are global measures of auroral electrojet activity (as is also the Dst index which measures global magnetospheric particle energy). To consider this aspect of geoeffectiveness, we chose a circle of magnetometers at different longitudes in a narrow MLAT band (60.9° - 66.0°). These would normally

be subauroral stations, but during disturbed periods they would be in the auroral zone. They give an idea of what "geoeffectiveness" means for the world's population, most of which lives at or below these latitudes. We return to this point in the discussion section.

The magnetometers chosen are Dawson (MLAT= 66°, MLT = UT - 10:34 hours), Island Lake (MLAT = 64.5°, MLT = UT - 06:35 hours), Pinawa (MLAT = 60.7°, MLT = UT - 06:41 hours), Halley (MLAT = -61.5°, MLT = UT - 02:42 hours), Pello (MLAT = 63.5°, MLT = UT + 02:50 hours) and Oulu (MLAT = 60.9°, MLT = UT + 02:55 hours). In Figures 7a, 7b, and 7c we show the horizontal component of the Earth's field measured by the stations for OCT95, JAN97, and MAY96, respectively. The shaded areas shows when the magnetic local time of the station in question is within ±3 hours of local midnight.

It is, of course, at this midnight region that the strongest magnetic activity is concentrated. Consequently, the local geoeffectiveness of the magnetic cloud depends greatly on the universal time of cloud arrival, e.g., compare geomagnetic disturbances at Halley and Pinawa during the $B_z < 0$ phase of the OCT95 cloud, or at Halley and Oulu during the MAY96 cloud. These data also emphasize that small differences in latitude can mean large differences in geoeffectivenss which rep-
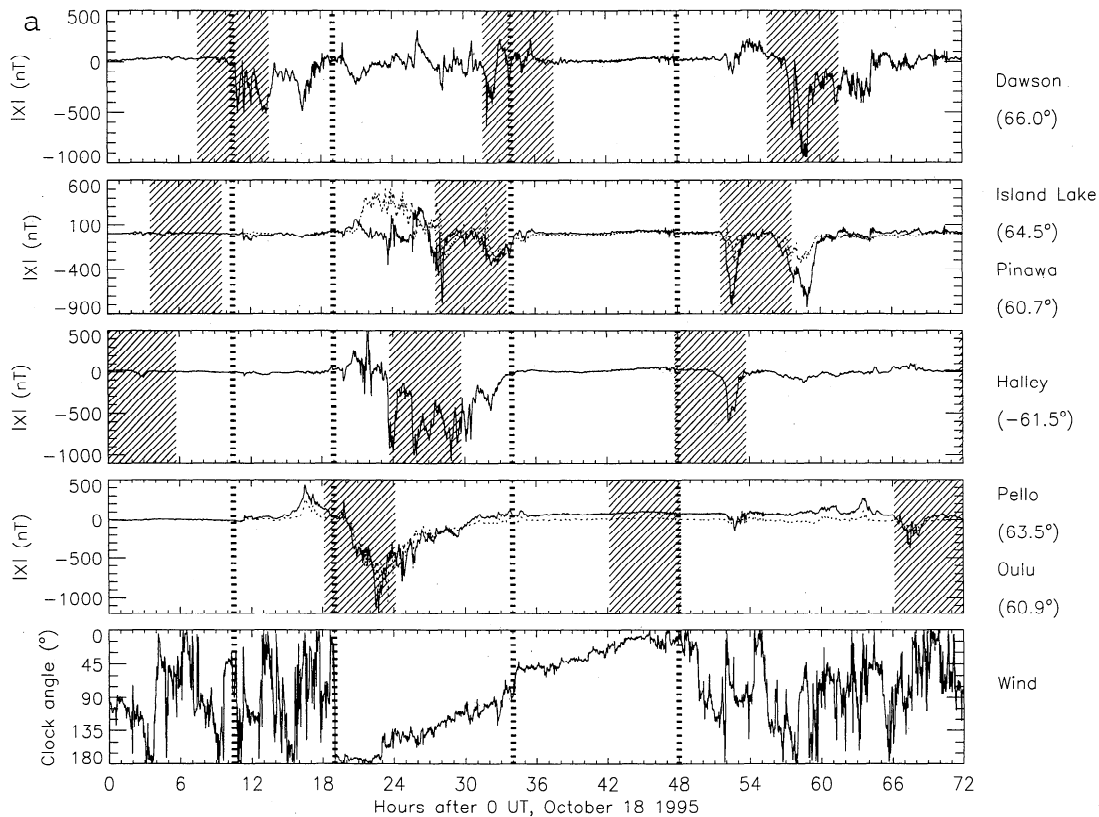

Figure 7. X component of the geomagnetic field at six stations along a narrow latitudinal band. The bottom panel shows the IMF clock angle seen at Wind, included for reference. The shaded areas indicate the universal times when the station are within ±3 hours of local magnetic midnight: (a) OCT95, (b) JAN97, and (c) MAY96.
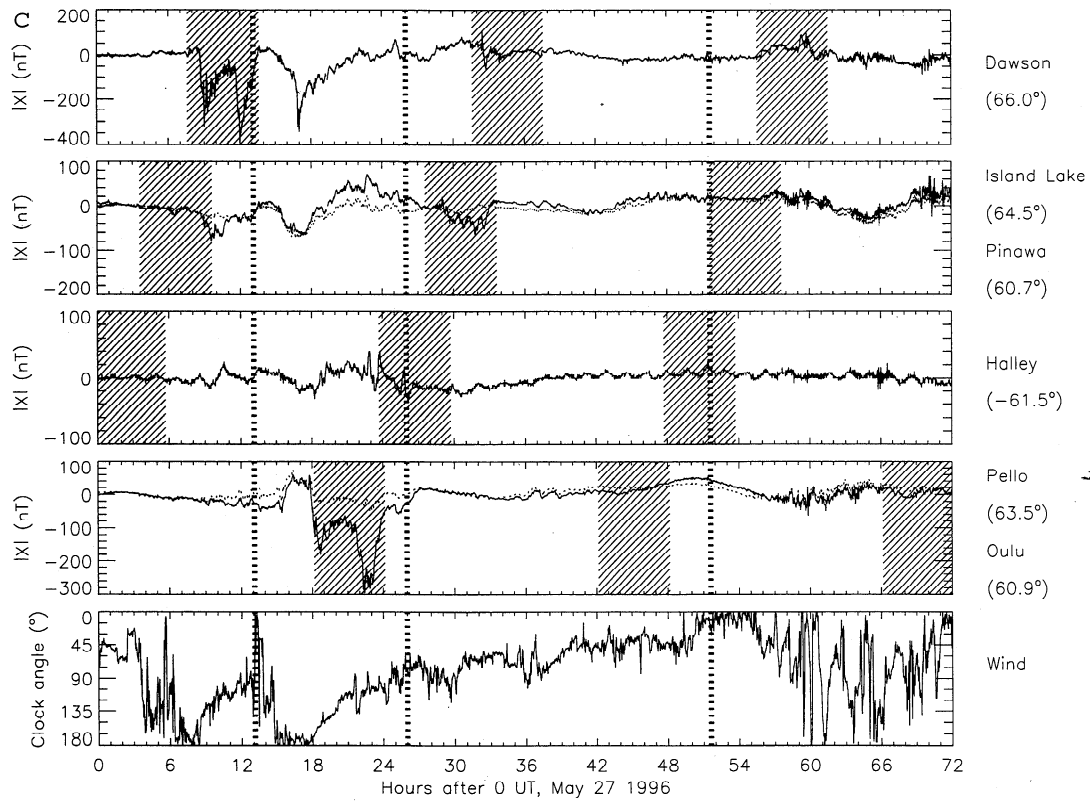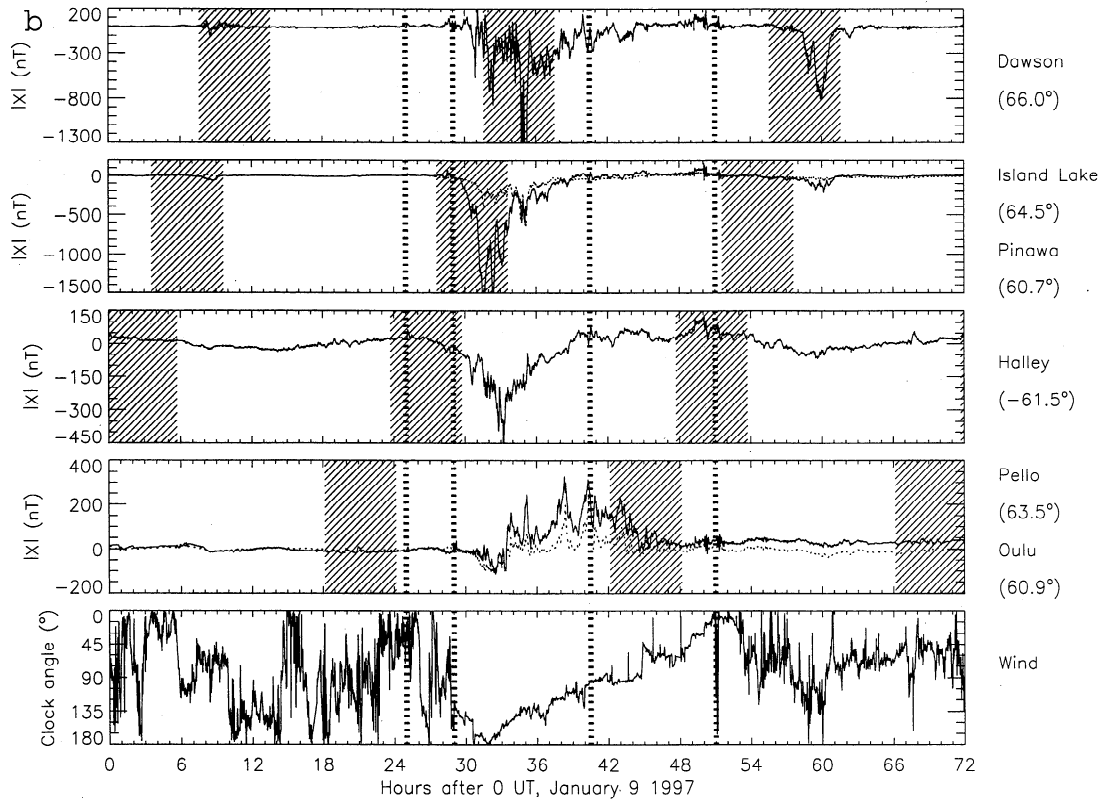
Figure 7. (continued)

resents a great forecasting challenge, e.g., compare Island Lake and Pinawa on OCT95 and Oulu and Pello on MAY96.

In summary, the comparison of these three magnetic clouds spells out the practical difficulties to be faced in combining the measureable solar wind input to the magnetosphere with the well-known localization of that energy within it to yield a reliable forcasting tool.

6. Discussion and Conclusions

The main points of this comparison of the geoeffects of three magnetic clouds observed by the Wind spacecraft in a ~15-month period around the minimum phase of the solar cycle may be summarized as follows:

1. The responses of the magnetosphere to cloud passage differ greatly from one cloud to the other. MAY96 elicited only weak, whereas JAN97 and, even more, OCT95 caused very disturbed geomagnetic conditions, as measured by ring current and auroral electrojet activity, and effects due to changes in dynamic pressure.

2. Despite these large differences in response, the temporal profiles of the interplanetary parameters were very similar, a circumstance which suggests that these configurations were generated in similar physical processes at the Sun.

3. We ascribed the different responses of the magnetosphere to differences in the temporal scale and amplitude of variation of quantities which past research has shown to be relevant to solar wind-magnetosphere coupling, such as duration and average size of the $B_z < 0$ phase, size, and impulsiveness of the dynamic pressure changes, etc. In how far these differences are intrinsic to the configurations or develop as the configurations evolve en route to Earth is an issue worth pursuing. Past work has shown that the thermodynamic and field signatures of magnetic clouds do evolve in time, and the evolution of isolated clouds has been followed and modeled over distances of several AU [Osherovich et al., 1993]. In the present case, one would expect the cloud-stream interaction to have developed and strengthened in transit from the Sun. Two probes in the upstream solar wind should be helpful in monitoring such evolutionary processes and extrapolating them to 1 AU.

4. The interaction of the individual clouds with the faster following streams leads to long intervals of strong, northward pointing fields. The possibility of reconnection tailward of the cusp arises. This was particularly the case for MAY97, where season, B_x polarity, and the long duration of an interval of very small IMF clock angles all favoured this possibility in the northern hemisphere. (However, reconnection tailward of the cusp, since it does not open closed flux, does not feature in the effects we studied.) There is the further possibility of exciting the Kelvin-Helmholtz instability at the dayside magnetopause, thought to be a major contributor to "viscous-type" interaction of the solar wind with the

magnetosphere. The interaction with the faster stream also weakened the control of the cloud's field on the flow in the Earth's magnetosheath.

5. We gave a counterexample to the criterion for the generation of major storms. This criterion was based on studies near solar maximum. Thus it is not possible to take this criterion over unreservedly to solar minimum conditions. The reason for this is not clear at present.

6. A unique feature of these Wind clouds is the suddennness of onset, characterized by a rapid decrease in the dynamic pressure, and a strong southward rotation of the field. Conditions at onset can thus be treated as a case of enhanced reconnection. The powering of the magnetosphere by the solar wind and accompanying geomagnetic effects typically occurred essentially within a few hours of cloud onset.

7. A point we made on the relevance to space weather efforts is the concentration of the energy from the solar wind to select parts of the globe, illustrating this by showing how strongly dependent on the universal time of cloud arrival (and whether a negative-positive or a positive-negative cloud phase comes first) auroral electrojet activity at a given station was.

In recent developments, attempts have been made at predicting the geoeffectiveness of magnetic clouds, modeled as cylindrical flux ropes, from solar observations of disappearing filaments, thought to be the source of these configurations [Zhao and Hoeksema, 1997, 1998]. So far, these studies have concentrated on predicting the strength and duration of the $B_z < 0$ interval from the direction of the axial field in the flux rope, and relating this direction to the orientation of the putative solar filament. While this approach is very promising, there are at present severe problems to overcome before a satisfactory prediction of geoeffects from solar observations can be achieved. Among these problems are that the inferred orientation of the flux rope in interplanetary space is totally model dependent [cf. Marubashi, 1997] and that the interaction with the medium has still to be adequately incorporated in studies of how erupting solar filaments evolve from Sun to Earth. In the examples we have discussed, the latter aspect is particularly crucial. Until these problems are solved, interplanetary monitor(s) are indispensable.

References

Akasofu, S.-I., Energy coupling between the solar wind and the magnetosphere, *Space Sci. Rev., 28*, 121, 1981.

Arnoldy, R. L., Signature in the interplanetary medium for substorms, *J. Geophys. Res., 76,* 5189, 1971.

Baker, D. N., R. D. Zwickl, S. J. Bame, E. W. Hones Jr., B. T. Tsurutani, E. J. Smith, and S.-I. Akasofu, An ISEE 3 high time resolution study of interplanetary parameter correlations with magnetospheric activity, *J. Geophys. Res., 88,* 6230, 1983.

Borovsky, J. E., M. F. Thomsen, and D. J. McComas, The superdense plasma sheet: Plasmaspheric origin, solar-wind origin, or ionospheric origin?, *J. Geophys. Res., 102,* 22,089, 1997.

Burlaga, L. F., Magnetic clouds, in *Physics of the Inner Heliosphere,* vol. 2, edited by R. Schwenn and E. Marsch, p. 1, Springer-Verlag, New York, 1991.

Burlaga, L. F., and R. P. Lepping, The causes of recurrent geomagnetic storms, *Planet. Space Sci., 25,* 1151, 1977.

Burlaga, L. F., E. Sittler, F. Mariani, and R. Schwenn, Magnetic loop behind an interplanetary shock: Voyager, Helios, and IMP observations, *J. Geophys. Res., 86,* 6673, 1981.

Burlaga, L. F., K. W. Behannon, and L. W. Klein, Compound streams, magnetic clouds, and major geomagnetic storms, *J. Geophys. Res., 92,* 5725, 1987.

Burlaga, L. F., et al., A magnetic cloud containing prominence material: January 1997, *J. Geophys. Res., 103,* 277, 1998.

Burton, R. K., R. L. McPherron, and C. T. Russell, An empirical relationship between interplanetary conditions and *Dst, J. Geophys. Res., 80,* 4204, 1975.

Cowley, S. W. H., Magnetospheric asymmetries associated with Y-component of the IMF, *Planet Space Sci., 29,* 79, 1981.

Cowley, S. W. H., J. P. Morelli, and M. Lockwood, Dependence of convective flows and particle precipitation in the high-latitude dayside ionosphere on the X and Y components of the interplanetary magnetic field, *J. Geophys. Res., 96,* 5557, 1991.

Crooker, N. U., Reverse convection, *J. Geophys. Res., 97,* 19,363, 1992.

Fairfield, D. H., Average and unusual locations of the Earth's magnetopause and bow shock, *J. Geophys. Res., 76,* 6700, 1971.

Fairfield, D. H., and L. J. Cahill Jr., Transition region magnetic field and polar magnetic disturbances, *J. Geophys. Res., 71,* 155, 1966.

Farrugia, C. J., N. V. Erkaev, H. K. Biernat, and L. F. Burlaga, Anomalous magnetosheath properties during Earth passage of an interplanetary magnetic cloud, *J. Geophys. Res., 100,* 19,245, 1995.

Farrugia, C. J., L. F. Burlaga, and R. P. Lepping, Magnetic clouds and the quiet-storm effect at Earth, in *Magnetic Storms, Geophys. Monogr. Ser.,* vol. 98, edited by B. T. Tsurutani, W. D. Gonzalez, and Y. Kamide, p. 91, AGU, Washington, D. C., 1997a.

Farrugia, C. J., N. V. Erkaev, H. K. Biernat, G. R. Lawrence, and R. C. Elphic, Plasma depletion layer model for low Alfven Mach number: Comparison with ISEE observations, *J. Geophys. Res., 102,* 11,315, 1997b.

Freeman, M. P., C. J. Farrugia, and S. W. H. Cowley, The response of dayside ionospheric convection to the Y-component of the magnetosheath magnetic field: A case study, *Planet. Space Sci., 38,* 13, 1990.

Freeman, M. P., C. J. Farrugia, L. F. Burlaga, M. Hairston, M. E. Greenspan, J. M. Ruohoniemi, and R. P. Lepping, The interaction of a magnetic cloud with Earth: Ionospheric convection in the northern and southern hemispheres for a wide range of quasi-steady interplanetary magnetic field conditions, *J. Geophys. Res., 98,* 7633, 1993.

Gonzalez, W. D, and B. T. Tsurutani, Criteria of interplanetary parameters causing intense magnetic storms ($Dst <$ -100 nT), *Planet. Space Sci., 35,* 1101, 1987.

Gosling, J. T., S. J. Bame, D. J. McComas, and J. L. Phillips, Coronal mass ejections and large geomagnetic storms, *Geophys. Res. Lett., 17,* 901, 1990.

Gosling, J. T., D. J. McComas, J. L. Phillips, and S. J. Bame, Geomagnetic activity associated with Earth passage of interplanetary shock disturbances and coronal mass ejections, *J. Geophys. Res., 96,* 7831, 1991.

Janoo, L., et al., Field and flow perturbations in the October 18-19, 1995 magnetic cloud, *J. Geophys. Res.,* in press, 1998.

Jordanova, V. K., J. U. Kosyra, A. F. Nagy, and G. V. Khazanov, Kinetic model of the ring current-atmosphere interactions, *J. Geophys. Res., 102,* 14,279, 1997.

Jordanova, V. K., C. J. Farrugia, L. Janoo, J. M. Quinn, R. B. Torbert, K. W. Ogilvie, R. P. Lepping, J. T. Steinberg, D. J. McComas, and R. D. Belian, The October 1995 magnetic cloud and accompanying storm activity: Ring current evolution, *J. Geophys. Res., 103,* 79, 1998.

Knipp, D. J., et al., Ionospheric convection response to slow, strong variations in a northward interplanetary magnetic field: A case study for January 14, 1988, *J. Geophys. Res., 98,* 19,273, 1993.

Lepping, R. P., M. H. Acuna, L. F. Burlaga, W. M. Farrell, J. A. Slavin, K. H. Schatten, F. Mariani, N. F. Ness, F. M. Neubauer, and Y. C. Whang, The WIND magnetic field investigation, *Space Sci. Rev., 71,* 207, 1995.

Lepping, R. P., L. F. Burlaga, A. Szabo, K. W. Ogilvie, W. H. Mish, D. Vassiliadis, A. J. Lazarus, J. T. Steinberg, C. J. Farrugia, L. Janoo, and F. Mariani, The WIND magnetic cloud and events of October 18 - 20, 1995: Interplanetary properties and as triggers for geomagnetic activity, *J. Geophys. Res., 102,* 14,049, 1997.

Marubashi, K., Interplanetary flux ropes and solar filaments, in *Coronal Mass Ejections, Geophys. Monogr. Ser.,* vol. 99, edited by N. U. Crooker, J. A. Joselyn, and J. Feynman, p. 147, AGU, Washington, D. C., 1997.

McPherron, R. L., Physical processes producing magnetospheric substorms and magnetic storms, in *Geomagnetism,* vol. 4, edited by J. A. Jacobs, Academic, San Diego, Calif., 1991.

Ogilvie, K. W., et al., SWE, A comprehensive plasma instrument for the WIND spacecraft, *Space Sci. Rev., 71,* 55, 1995.

Osherovich, V. A., C. J. Farrugia, and L. F. Burlaga, Dynamics of aging magnetic clouds, *Adv. Space Res., 13,* 6(6), 57, 1993.

Paschmann, G., I. Papamastorakis, W. Baumjohann, N. Sckopke, C. W. Carlson, B. U. O. Sonnerup, and H. Luehr, The magnetopause for large magnetic shear: AMPTE/IRM observations, *J. Geophys. Res., 91,* 11,099, 1986.

Perreault, P., and S.-I. Akasofu, A study of geomagnetic storms, *Geophys. J. R. Astron. Soc., 54,* 547, 1978.

Petrinec, S. M., and C. T. Russell, External and internal influences on the size of the dayside terrestrial magnetosphere, *Geophys. Res. Lett., 20,* 339, 1993.

Phan, T.-D., G. Paschmann, and B. U. O. Sonnerup, low-latitude dayside magnetopause and boundary layer for high magnetic shear, 2, Occurrence of magnetic reconnection, *J. Geophys. Res., 101,* 7817, 1996.

Rosenberg, T. J., et al., Observations during passage on May 27, 1996 of a magnetic hole in front of a magnetic cloud: A coordinated ground and spacecraft study, *Eos Trans. AGU, 77,* Fall Meet. Suppl., F633, 1996.

Scudder, J. D., et al., Separatrix crossings and possible penetration of the diffusion region in an example of recon-

nection, poleward of the cusp, *Eos Trans. AGU, 77,* Fall Meet. Suppl., F617, 1996.

Snyder, C. W., M. Neugebauer, and U. R. Rao, The solar wind velocity and its correlation with cosmic ray variation and with solar and geomagnetic activity, *J. Geophys. Res., 68,* 6361, 1963.

Stern, D. P., Energetics of the magnetosphere, *Space Sci. Rev., 39,* 193, 1984.

Tsurutani, B. T., and W. D. Gonzalez, The cause of high-intensity long-duration continuous *AE* activity (HILD-CAAs): Interplanetary Alfven wave trains, *Planet. Space Sci., 35,* 405, 1987.

Tsurutani, B. T., and W. D. Gonzalez, The interplanetary causes of magnetic storms: A review, in *Magnetic Storms, Geophys. Monogr. Ser.,* vol. 98, edited by B. T. Tsurutani, W. D. Gonzalez, and Y. Kamide, p. 77, AGU, Washington, D. C., 1997.

Tsurutani, B. T., W. D. Gonzalez, F. Tang, S-I. Akasofu, and E. J. Smith, Origin of interplanetary southward magnetic fields responsible for major magnetic storms near solar maximum (1978-1979), *J. Geophys. Res., 93,* 8519, 1988.

Tsurutani, B. T., W. D. Gonzalez, A. L. C. Gonzalez, F. Tang, J. K. Arballo, and M. Okada, Interplanetary origin of geomagnetic activity in the declining phase of the solar cycle, *J. Geophys. Res., 100,* 21,717, 1995.

Villante, U., M. DeLauretis, P. Francia, S. Lepidi, E. Pietropaolo, L. Cafarella, A. J. Lazarus, R. P. Lepping, and F. Mariani, The Earth's passage of a magnetic cloud on January 10-11, 1997: A preliminary analysis of geomagnetic field fluctuations at a low latitude and an antactic station, in *Proceedings Cosmic Physics in the Year 2000 ,* vol. 58, p. 147, SIF, Bologna, 1997.

Wilson, R. M., Geomagnetic response to magnetic clouds, *Planet. Space Sci., 35,* 329, 1987.

Wilson, R. M., On the behavior of the Dst geomagnetic index in the vicinity of magnetic cloud passage at Earth, *J. Geophys. Res., 95,* 215, 1990.

Zhang, G., and L. F. Burlaga, Magnetic clouds, geomagnetic disturbances, and cosmic ray decreases, *J. Geophys. Res., 93,* 2511, 1988.

Zhao, X. P., and J. T. Hoeksema, Is the geoeffectiveness of the 6 January 1997 CME predictable from solar observations?, *Geophys. Res. Lett., 24,* 2965, 1997.

Zhao, X. P., and J. T. Hoeksema, Central axial field direction in magnetic clouds and its relation to southward interplanetary magnetic field events and dependence on disappearing solar filaments, *J. Geophys. Res., 103,* 2077, 1998.

R. L. Arnoldy, C. J. Farrugia, L. Janoo, J. M. Quinn, and R. B. Torbert, Institute for the Study of Earth, Oceans, and Space, University of New Hampshire, Morse Hall, Durham, NH 03820.(e-mail: farrugia@monet.sr.unh.edu)

L. F. Burlaga, R. P. Lepping, K. W. Ogilvie, NASA Goddard Space Flight Center, Code 692, Greenbelt, MD 20771.

M. P. Freeman, British Antarctic Survey, High Cross, Madingley Road, Cambridge, CB3 0ET, United Kingdom.

F. T. Gratton, Instituto de Fisica del Plasma, Universidad de Buenos Aires, Ciudad Universitaria, Pabellon 1, 1428 Buenos Aires, Argentina.

A. J. Lazarus and J. T. Steinberg, Massachusetts Institute of Technology, Cambridge, MA 02139.

G. Lu, High Altitude Observatory, NCAR, Boulder, CO 80307.

G. Rostoker, Department of Physics, University of Alberta, Edmonton, AB T6G 2J1, Canada.

J. D. Scudder, Department of Physics and Astronomy, University of Iowa, Iowa City, IA 52240.